

PRIVACY-PRESERVING INDOOR LOCALIZATION VIA LIGHT TRANSPORT ANALYSIS

Jinyuan Zhao, Prakash Ishwar, and Janusz Konrad

Department of Electrical and Computer Engineering, Boston University, Boston, MA 02215

ABSTRACT

We propose a system for indoor localization using intensity-controllable LED light fixtures and light sensors mounted on the ceiling. While providing accurate location estimates, our approach preserves user privacy and is robust to ambient light conditions. We develop a LASSO algorithm and a localized ridge regression algorithm for locating a single object. In synthetic experiments, our localized ridge regression algorithm achieves an average localization error ranging from 0.24in to 1.39in, for different object sizes, in a 7×12 -foot room. The localized ridge regression algorithm also shows the ability to locate multiple objects in experiments with a real-world occupancy scenario.

Index Terms— Indoor localization, LASSO, light transport analysis, ridge regression

1. INTRODUCTION

Indoor localization is a key step in many location-based applications for indoor environments. These include human tracking, location-based Internet access, indoor navigation, surveillance, occupancy-based lighting and HVAC control, etc. In the context of smart rooms, accurate indoor localization is expected to help save energy, improve productivity, and offer health benefits.

Various systems have been designed for indoor localization [1]. While GPS [2] works well outdoors, it is not robust for indoor localization. Active systems, that require users to wear an electronic device, e.g., Active Badge Location [3], *Cricket* [4], SpotON [5], and LANDMARC [6], are intrusive and are not user friendly. Passive systems do not require a user to wear an active device. Instead, they exploit, for example, WiFi signals [7, 8, 9] or air flow [10]. However, they require a sufficiently strong signature (disruption of WiFi signal or air flow), and their performance is easily affected by environmental noise and signal reflections off walls, furniture, etc. Localization can be also performed using visual and auditory cues via multi-camera systems, e.g., *EasyLiving Tracker* [11], W^4 [12], W^4S [13], and Hydra [14], single-camera systems [15], or microphone arrays [16]. While such systems provide accurate localization, they raise privacy concerns on account of image and/or voice capture.

Recently, indoor localization methods that preserve user

privacy have been proposed. One common approach is by degrading data, either optically prior to capture by the sensor [17] or digitally, post-capture [18]. While the first method requires manipulation of optics and results in very limited range of degradations, the other method is susceptible to eavesdropping prior to degradation. An alternative is to use ultra-low resolution sensors. Jia and Radke [19] developed a privacy-preserving person localization, tracking and coarse pose estimation system with ceiling-mounted time-of-flight (ToF) sensors. They showed that their algorithm works effectively for 0.25m sensor spacing, in both real and simulated environments. Wang *et al.* [20] proposed a system to estimate room occupancy using LED light fixtures and color sensors. They proposed a light blockage model for 3D occupancy estimation with wall-mounted sensors, and a light reflection model for 2D floor-plane occupancy estimation with ceiling-mounted sensors. In the light reflection model, they add perturbations to the inputs of light fixtures and estimate an occupancy “confidence map” using light reflected by the floor.

In this paper, we develop an indoor localization algorithm based on floor-reflected light transport analysis that can accurately locate an object in a room while preserving user privacy. To this end, we revisit Wang *et al.*’s light reflection model [20] and propose two *principled* localization algorithms that are able to locate a single object. We prove the effectiveness of our algorithms *via* both synthetic and real-world experiments.

2. ALGORITHM

2.1. Light Reflection Model

Wang *et al.*’s light reflection model [20] is an active light sensing model that uses both reflected light measurements and light source modulation information (Fig. 1). In this model, the ceiling-mounted LED fixtures provide maximum light intensity I_{\max} in the vertical direction, and the light intensity at angle θ to the normal direction is $I_{\max}q(\theta)$, where $q(\theta)$ is the intensity distribution function, shown in Fig. 2.

For an LED fixture number j and a small area dS_1 on the floor plane at location s , the luminous flux arriving at dS_1 is:

$$\Phi_1(j; s) = x(j)I_{\max}q(\theta_1) \frac{dS_1 \cos \theta_1}{4\pi D_1^2}.$$

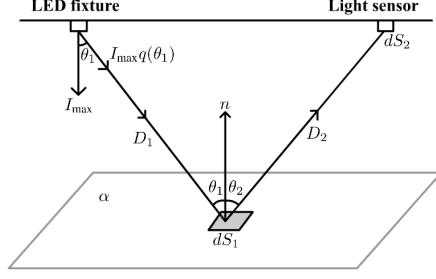


Fig. 1. Light reflection model proposed by Wang *et al.* [20]

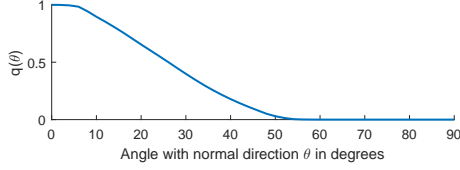


Fig. 2. Light intensity distribution function $q(\theta)$.

where $x(j)$ is the relative intensity of source j , scaled to the range $[0, 1]$, while $\frac{dS_1 \cos \theta_1}{4\pi D_1^2}$ is a solid angle from the LED fixture to area dS_1 . Note that θ_1 and D_1 are functions of j and s , but for convenience of notation we omit this dependence.

We assume that the light reflected by the floor obeys the Lambert's cosine law, the light sensor has an area of dS_2 , and the floor has albedo $\alpha(s)$ at location s . Then, the luminous flux received by sensor number i is:

$$\Phi_2(i, j; s) = \alpha(s) \Phi_1(j; s) \cos \theta_2 \frac{dS_2 \cos \theta_2}{4\pi D_2^2} \quad (1)$$

where θ_2 and D_2 are again functions of i and s . By defining

$$C(i, j; s) = \frac{\Phi_2(i, j; s)}{x(j)\alpha(s)dS_1},$$

which only depends on the room geometry, we can express the total flux at sensor i produced by unit flux from source j as follows:

$$A(i, j) = \int_{S_F} \alpha(s) C(i, j; s) ds \quad (2)$$

where S_F is the whole floor plane.

2.2. Light Transport Model

In a room with N_f light fixtures and N_s sensors, there is a linear relationship between fixture outputs and sensor outputs:

$$\mathbf{y} = \mathbf{A}\mathbf{x} + \mathbf{b}$$

where \mathbf{x} is an $N_f \times 1$ vector of intensities $x(j)$ from all LED fixtures, \mathbf{y} is an $N_s \times 1$ vector of all sensor outputs, \mathbf{b} is an $N_s \times 1$ vector accounting for the effects of ambient light, and

\mathbf{A} is an $N_s \times N_f$ light transport matrix [20] whose ij -th entry is $A(i, j)$ defined in (2).

A change in the room state (change in albedo $\alpha(s)$) leads to a change in matrix \mathbf{A} . To estimate the location of the change, we need to recover matrix \mathbf{A} . We assume that \mathbf{b} is a constant vector since ambient light changes slowly compared to the modulation-response time. In order to recover \mathbf{A} , we need to induce at least N_f linearly-independent perturbations $\Delta \mathbf{x}$ in \mathbf{x} , and measure the corresponding changes in sensor outputs $\Delta \mathbf{y}$. Let $\Delta \mathbf{X} = [\Delta \mathbf{x}_1, \dots, \Delta \mathbf{x}_n]$ and $\Delta \mathbf{Y} = [\Delta \mathbf{y}_1, \dots, \Delta \mathbf{y}_n]$ where $n \geq N_f$. Then, the least squares solution for A is given by [20]:

$$\mathbf{A} = \Delta \mathbf{Y} \Delta \mathbf{X}^T (\Delta \mathbf{X} \Delta \mathbf{X}^T)^{-1}.$$

2.3. LASSO Algorithm

Suppose that we have obtained two light transport matrices: \mathbf{A}_0 for the initial state (e.g., empty room) and \mathbf{A} for a new state (e.g., object in the room). If we take the difference $\mathbf{E} = \mathbf{A} - \mathbf{A}_0$ and use equation (2), we obtain:

$$\mathbf{E}(i, j) = \int_{S_F} \Delta \alpha(s) C(i, j; s) ds \quad (3)$$

where $\Delta \alpha(s)$ is the change of albedo between the two states. Assuming that objects are flat, $\Delta \alpha(s)$ characterizes the location and size of the introduced object. We discretize equation (3) by assuming that the room's width is W , its length is L and the quantization step is δ , thus leading to:

$$\mathbf{e} = \delta^2 \mathbf{C} \Delta \alpha \quad (4)$$

where \mathbf{e} is a vector of length $N_f \times N_s$ formed by scanning matrix \mathbf{E} , \mathbf{C} is a matrix with $N_f \times N_s$ rows and $\lfloor \frac{W}{\delta} \rfloor \times \lfloor \frac{L}{\delta} \rfloor$ columns obtained by scanning $C(i, j; s)$, and $\Delta \alpha$ is a vector of length $\lfloor \frac{W}{\delta} \rfloor \times \lfloor \frac{L}{\delta} \rfloor$ with each entry corresponding to a point on the discretized floor grid (location s).

Generally, the area of change is small compared to the floor size, so it is reasonable to assume that $\Delta \alpha$ is a sparse vector. Inspired by LASSO regression, we first solve for $\Delta \alpha$ the following convex optimization problem with l_1 penalty:

$$\arg \min_{\Delta \alpha} \|\mathbf{e} - \delta^2 \mathbf{C} \Delta \alpha\|_{l_2}^2 + \lambda \delta^2 \|\Delta \alpha\|_{l_1}, \quad (5)$$

where λ is a tuning parameter. Then, in order to estimate the location of the change, we compute the centroid of the magnitude of $\Delta \alpha$:

$$\begin{aligned} \text{Loc}_x &= \frac{\sum_k \text{Loc}_x(k) |\Delta \alpha(s_k)|}{\sum_k |\Delta \alpha(s_k)|} \\ \text{Loc}_y &= \frac{\sum_k \text{Loc}_y(k) |\Delta \alpha(s_k)|}{\sum_k |\Delta \alpha(s_k)|} \end{aligned} \quad (6)$$

where $\text{Loc}_x(k)$ and $\text{Loc}_y(k)$ are the x and y coordinates of the k -th point on the discretized floor (at location s_k).

2.4. Localized Ridge Regression Algorithm

We also propose to solve for $\Delta\alpha$ via a two-step approach. This method is a principled refinement of Wang *et al.*'s floor plane occupancy confidence map [20], defined as follows:

$$\text{map}(s) = \frac{\sum_{i=1}^{N_s} \sum_{j=1}^{N_f} E(i, j) C(i, j; s)}{\left(\sum_{i=1}^{N_s} \sum_{j=1}^{N_f} C(i, j; s)\right)} \quad (7)$$

which holds when the floor albedo is uniform. The confidence map is an ℓ_1 -normalized correlation between the columns of C (corresponding to different floor locations) and E . It provides coarse information about the floor-plane occupancy distribution. A high value in the confidence map at some location implies that this location is occupied with large probability, and vice versa.

First, we calculate the confidence map on the discretized floor plane. Then, in the second step, we perform ridge regression in an area S_{local} where the confidence map value is above a threshold (area that is more likely to be occupied):

$$\arg \min_{\Delta\alpha_{\text{local}}} \|\mathbf{e} - \delta^2 \mathbf{C}_{\text{local}} \Delta\alpha_{\text{local}}\|_{l_2}^2 + \sigma \delta^2 \|\Delta\alpha_{\text{local}}\|_{l_2}^2, \quad (8)$$

where $\mathbf{C}_{\text{local}}$ contains columns of \mathbf{C} corresponding to points inside S_{local} , and σ is a tuning parameter. We obtain a closed-form solution by setting the gradient to zero. The final solution $\Delta\alpha$ is equal to $\Delta\alpha_{\text{local}}$ inside S_{local} and 0 elsewhere.

3. EXPERIMENTAL RESULTS

3.1. Synthetic Data

We simulated a cuboid room in MATLAB. The room is 85.5in wide, 135.0in long and 86.4in tall [20]. We placed 12 LED light fixtures and 12 light intensity sensors on the ceiling of the simulated room. The light intensity of LED fixtures is continuously adjustable between zero and some maximum intensity. The floor albedo is assumed to be uniform at $\alpha = 0.5$. We also assume that there is no reflection by the walls or the ceiling, and no direct light path from fixtures to sensors.

In each experiment, we placed a square object on the floor. The object is Lambertian with albedo $\alpha = 0.9$. We discretized the floor with quantization step $\delta = 1$. For each occupancy scenario (before and after change), we generated 13 fixture input vectors \mathbf{x} (base light and 12 perturbations), and calculated the corresponding sensor output vectors \mathbf{y} , so that we obtain 12 $(\Delta x, \Delta y)$ pairs, enough to recover the light transport matrix \mathbf{A} . Each entry of \mathbf{x} is a random number uniformly distributed in $[0, 1]$ range.

The tuning parameter λ (or σ) was chosen to optimize the performance for each method. In the localized ridge regression algorithm, the threshold to identify S_{local} was set to $0.75 \times \max(\text{confidence map})$.

We evaluated the performance of both algorithms in terms of the localization error defined as the Euclidean distance between the ground-truth location (the geometric center of the

object) and the estimated location (6). A sample ground-truth location, the estimated confidence map (7) and the results of the LASSO and localized ridge regression algorithms are shown in Fig. 3.

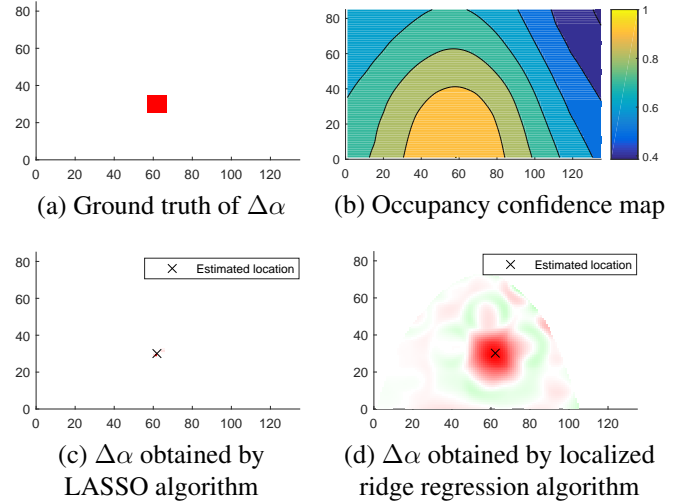


Fig. 3. Sample ground-truth location, estimated confidence map, and the results of LASSO and localized ridge regression algorithms. Red: positive $\Delta\alpha$, green: negative $\Delta\alpha$.

We have performed numerous experiments with different object sizes. For each object size, we repeated the experiment 100 times; the location of the object among the 100 tries was uniformly distributed on the floor plane. Table 1 shows the average localization error of the LASSO and localized ridge regression algorithms, as well as those obtained using the maximum and the centroid of the confidence map.

We note that both the LASSO and localized ridge regression algorithms perform better than localization with the confidence map in terms of localization error. The localized ridge regression algorithm has the best overall performance.

Fig. 4 compares the average running times of the LASSO and localized ridge regression algorithms. The localized ridge regression algorithm runs much faster than the LASSO algorithm because it has a closed-form solution which can be computed directly without using a gradient descent algorithm that involves initialization and iterations.

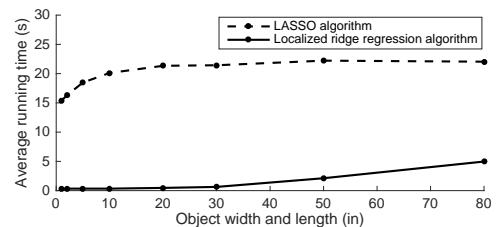


Fig. 4. Average running time with respect to object size.

Table 1. Average localization error for different object sizes.

Method	Object width and length [in]							
	1	2	5	10	20	30	50	80
LASSO	11.0131	6.0740	1.1698	0.3877	0.4203	0.3702	0.3746	0.4018
Localized ridge regression	0.6870	0.7096	0.5978	0.4255	0.2438	0.4790	1.3901	0.3264
Maximum of confidence map	26.3846	27.3360	27.7620	28.1792	31.2101	33.6728	36.2543	32.8679
Centroid of confidence map	24.9388	24.4359	23.6096	22.0416	19.7851	17.2605	13.2965	8.0171

3.2. Real Data

We also performed experiments on real data recorded in a LESA testbed¹. The testbed room has the same size as the simulated room, with 12 color-controllable LED fixtures and 12 optical light sensors on the ceiling. Each LED fixture has 3 color channels (R,G,B) with adjustable intensity, and each color sensor has 4 output channels (R,G,B, Unfiltered white). Two datasets are available: one recorded when the room is empty and one when it is occupied. In the latter scenario, two people and a chair occupy one side of the room (Fig. 5).



Fig. 5. Four views of the LESA testbed occupied by 2 people and a chair [20].

Our algorithm uses only intensity values that we extract from RGB channels similarly to Wang *et al.* [20] as follows. While matrix \mathbf{E} in (3) considers only single-channel fixtures and sensors, and thus is of dimension $N_s \times N_f$, in the LESA testbed we have 3-channel fixtures and 4-channel sensors. Therefore, in this case the \mathbf{E} matrix is of dimension $4N_s \times 3N_f$. We aggregate this multi-channel matrix \mathbf{E} into a single-channel matrix $\hat{\mathbf{E}}$ of dimension $N_s \times N_f$ by summing up those entries in \mathbf{E} that correspond to the impact of a certain color channel of an LED fixture on the same color channel of a color sensor (i.e., R-R, G-G and B-B) and ignoring the unfiltered white channel. Subsequently, we applied the localized ridge regression algorithm to the aggregated matrix $\hat{\mathbf{E}}$. The

¹The testbed is located at NSF’s Lighting Enabled Systems and Applications (LESA) Engineering Research Center (Rensselaer Polytechnic Institute, Boston University, University of New Mexico).

results are shown in Fig. 6.

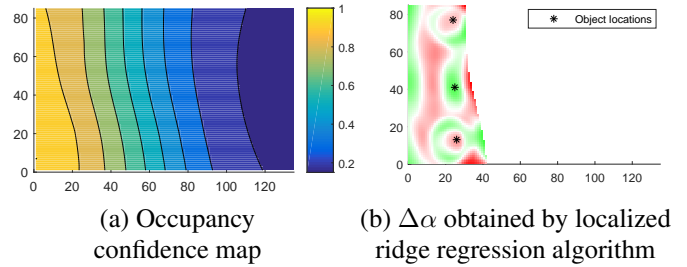


Fig. 6. Confidence map and the result of the localized ridge regression algorithm on real data. Red: positive $\Delta\alpha$, green: negative $\Delta\alpha$.

The $\Delta\alpha$ pattern in Fig. 6(b) shows three blobs corresponding to three objects (two people and a chair) present in the room. By finding the local maximum (minimum) of each blob, we estimated the location of each object. Note that while the confidence map in Fig. 6(a) shows a high likelihood (“hot” area – yellow) of occupancy at the left edge of the floor plane, the localized ridge regression algorithm has found precise locations of 3 objects consistent with the actual room occupancy (Fig. 5).

4. DISCUSSION AND CONCLUSION

We proposed an indoor localization system using 12 LED light fixtures and 12 visible light sensors mounted on the ceiling. Based on the light reflection model developed by Wang *et al.* [20], we proposed two improved ways of locating an object: one based on LASSO and one based on localized ridge regression. In synthetic experiments, these two approaches perform significantly better than localization using the confidence map proposed by Wang *et al.* For object sizes ranging in width and length from 1in to 80in, the localized ridge regression algorithm achieves an average localization error ranging from 0.24in to 1.39in. In a real-world experiment, where a room is occupied by two people and a chair, the localized ridge regression algorithm was able to precisely locate all three objects. With the use of LED fixtures and light sensors, our system is cheap to build and does not violate user privacy. Future work will consider extensions to multiple-object localization, object size estimation and incorporation of object height.

5. REFERENCES

- [1] Gabriel Deak, Kevin Curran, and Joan Condell, "A survey of active and passive indoor localisation systems," *Computer Communications*, vol. 35, no. 16, pp. 1939–1954, 2012.
- [2] Garmin Corporation, "About gps," <http://www.garmin.com/aboutGPS/>.
- [3] Roy Want, Andy Hopper, Veronica Falcao, and Jonathan Gibbons, "The active badge location system," *ACM Transactions on Information Systems (TOIS)*, vol. 10, no. 1, pp. 91–102, 1992.
- [4] Nissanka B Priyantha, Anit Chakraborty, and Hari Balakrishnan, "The cricket location-support system," in *Proceedings of the 6th annual international conference on Mobile computing and networking*. ACM, 2000, pp. 32–43.
- [5] Jeffrey Hightower, Roy Want, and Gaetano Borriello, "Spoton: An indoor 3d location sensing technology based on rf signal strength," *UW CSE 00-02-02, University of Washington, Department of Computer Science and Engineering, Seattle, WA*, vol. 1, 2000.
- [6] Lionel M Ni, Yunhao Liu, Yiu Cho Lau, and Abhishek P Patil, "Landmarc: indoor location sensing using active rfid," *Wireless networks*, vol. 10, no. 6, pp. 701–710, 2004.
- [7] May Moussa and Moustafa Youssef, "Smart ceives for smart environments: Device-free passive detection in real environments," in *Pervasive Computing and Communications, 2009. PerCom 2009. IEEE International Conference on*. IEEE, 2009, pp. 1–6.
- [8] Moustafa Youssef, Matthew Mah, and Ashok Agrawala, "Challenges: device-free passive localization for wireless environments," in *Proceedings of the 13th annual ACM international conference on Mobile computing and networking*. ACM, 2007, pp. 222–229.
- [9] Ahmed E Kosba, Ahmed Abdelkader, and Moustafa Youssef, "Analysis of a device-free passive tracking system in typical wireless environments," in *2009 3rd International Conference on New Technologies, Mobility and Security*. IEEE, 2009, pp. 1–5.
- [10] John Krumm, *Ubiquitous computing fundamentals*, CRC Press, 2016.
- [11] Microsoft Research, "Easy living," 2011, <http://www.research.microsoft.com>.
- [12] Ismail Haritaoglu, David Harwood, and Larry S. Davis, "W 4: Real-time surveillance of people and their activities," *IEEE Transactions on pattern analysis and machine intelligence*, vol. 22, no. 8, pp. 809–830, 2000.
- [13] Ismail Haritaoglu, David Harwood, and Larry S Davis, "W4s: A real-time system for detecting and tracking people in 2 1/2d," in *European Conference on computer vision*. Springer, 1998, pp. 877–892.
- [14] Ismail Haritaoglu, David Harwood, and Larry S Davis, "Hydra: Multiple people detection and tracking using silhouettes," in *Image Analysis and Processing, 1999. Proceedings. International Conference on*. IEEE, 1999, pp. 280–285.
- [15] Romer Rosales and Stan Sclaroff, "3d trajectory recovery for tracking multiple objects and trajectory guided recognition of actions," in *Computer Vision and Pattern Recognition, 1999. IEEE Computer Society Conference on*. IEEE, 1999, vol. 2.
- [16] Qian Huang, Zhenhao Ge, and Chao Lu, "Occupancy estimation in smart buildings using audio-processing techniques," *arXiv preprint arXiv:1602.08507*, 2016.
- [17] Francesco Pittaluga and Sanjeev J Koppal, "Privacy preserving optics for miniature vision sensors," in *Proceedings of the IEEE Conference on Computer Vision and Pattern Recognition*, 2015, pp. 314–324.
- [18] Adám Erdélyi, Tibor Barát, Patrick Valet, Thomas Winkler, and Bernhard Rinner, "Adaptive cartooning for privacy protection in camera networks," in *Advanced Video and Signal Based Surveillance (AVSS), 2014 11th IEEE International Conference on*. IEEE, 2014, pp. 44–49.
- [19] Li Jia and Richard J Radke, "Using time-of-flight measurements for privacy-preserving tracking in a smart room," *IEEE Transactions on Industrial Informatics*, vol. 10, no. 1, pp. 689–696, 2014.
- [20] Quan Wang, Xinchu Zhang, and Kim L Boyer, "Occupancy distribution estimation for smart light delivery with perturbation-modulated light sensing," *Journal of solid state lighting*, vol. 1, no. 1, pp. 1, 2014.